

# Amphiphile-induced anisotropic colloidal self-assembly

*Marcel Rey<sup>a,‡</sup>, Taotao Yu<sup>a,‡</sup>, Karina Bley<sup>a,b</sup>, Katharina Landfester<sup>b</sup>, D. Martin A. Buzza<sup>c</sup>,  
Nicolas Vogel<sup>a,\*</sup>*

<sup>a</sup> Institute of Particle Technology, Friedrich-Alexander University Erlangen-Nürnberg,  
Cauerstrasse 4, 91058 Erlangen, Germany

<sup>b</sup> Max Planck Institute for Polymer Research, Ackermannweg 10, 55128 Mainz, Germany

<sup>c</sup> G W Gray Centre for Advanced Materials, School of Mathematics & Physical Sciences,  
University of Hull, Hull HU6 7RX, United Kingdom

This document is the Accepted Manuscript version of a Published Work that appeared in final form in *Langmuir*, copyright © American Chemical Society after peer review and technical editing by the publisher. To access the final edited and published work see

<https://pubs.acs.org/doi/10.1021/acs.langmuir.8b01382>

Abstract:

Spherical colloidal particles typically self-assemble into hexagonal lattices when adsorbed at liquid interfaces. More complex assembly structures, including particle chains and phases with square symmetry, were theoretically predicted almost two decades ago for spherical particles interacting via a soft repulsive shoulder. Here, we demonstrate that such complex assembly phases can be experimentally realized with spherical colloidal particles assembled at the air/water interface in the presence of molecular amphiphiles. We investigate the interfacial behavior of colloidal particles in the presence of different amphiphiles on a Langmuir trough. We transfer the structures formed at the interface onto a solid substrate while continuously compressing, which enables us to correlate the prevailing assembly phase as a function of the available interfacial area. We observe that block-copolymers with similarities to the chemical nature of the colloidal particles, as well as the surface-active protein bovine serum albumin direct the colloidal particles into complex assembly phases, including chains and square arrangements. The observed structures are reproduced by minimum energy calculations of hard core-soft shoulder particles with experimentally realistic interaction parameters. From the agreement between experiments and theory, we hypothesize that the presence of the amphiphiles effectively manipulates the interaction potential of the colloidal particles. The assembly of spherical colloidal particles into complex assembly phases on solid substrates opens new possibilities for surface patterning by enriching the library of possible structures available for colloidal lithography.

## Introduction

Colloidal particles are useful building blocks to fundamentally study self-assembly phenomena<sup>1-4</sup> as well as to engineer functional materials with a defined structure at the nanoscale.<sup>5-7</sup>

When adsorbed at a liquid interface, colloids are able to crystallize into ordered two-dimensional lattices.<sup>1,8,9</sup> Depending on the balance between attractive van der Waals and capillary forces (arising from contact line undulations<sup>10</sup>) and repulsive electrostatic and dipole forces, monodisperse spherical colloidal particles typically form close packed or non-close packed arrangements with hexagonal symmetry.<sup>3,11</sup>

These colloidal monolayers can be deposited onto a solid substrate, providing a strategy to create ordered nanoscale surface patterns in a simple and fast process over macroscopic dimensions. The deposited colloidal particles can further serve as templates and shadow- or etching masks to create more complex surface nanostructures, used for example in photonics,<sup>12-15</sup> phononics,<sup>16,17</sup> electronics,<sup>18,19</sup> liquid repellency<sup>20,21</sup> or to control cell-surface interactions.<sup>22,23</sup> However, the tendency of spherical colloidal particles to assemble into hexagonal lattices limits the available structural motifs for such surface nanostructures.

Ongoing research efforts therefore focus on manipulating the self-assembly process to create colloidal surface patterns with more complex symmetries. Changing the shape of the colloidal building blocks to cubic or octahedral enables the assembly of square lattices as the densest packing.<sup>24,25</sup> Introducing defined patches on spherical colloidal particles is another way to manipulate the symmetry of the assembly.<sup>26,27</sup> Manipulating the interaction potential by external electric<sup>28-30</sup> or magnetic fields<sup>31-33</sup> may induce dipoles and align the particles into chains oriented along the field lines. Similarly, the directionality of the capillary interaction forces can be manipulated with anisotropic particles<sup>34,35</sup> or a defined curvature of the liquid interface<sup>36,37</sup> to create square symmetries or particle chains. Further, liquid crystal interfaces can guide spherical colloids into 1D chains or 2D crystals.<sup>38,39</sup> Topographically prestructured

surfaces provide an alternative engineering to guide the assembly of colloids.<sup>40-42</sup> Common to all of these approaches is that the anisotropy of the final assembly is externally imposed onto the colloidal particles via process conditions, force fields, or the properties of the substrate.

Nearly two decades ago, Jagla predicted that even spherical particles with an isotropic interaction potential are able to assemble into anisotropic structures when confined in two dimensions.<sup>43,44</sup> The formation of such complex phases requires an isotropic repulsive interaction potential with two distinct length scales, consisting of a hard sphere potential at the particle core and a longer repulsive shoulder. **When forced into contact by increase of the particle density, such systems minimize their free energy by fully overlapping their shells in some directions in order to avoid overlap in other directions.**<sup>43,45-47</sup> As a result, chain structures, square symmetries or even more complex structural motifs including quasi-crystals have been theoretically predicted as minimum free energy phases.<sup>47-52</sup>

Recently, we devised an experimental system that showed structural similarities to the theoretical predictions by Jagla. We co-assembled spherical, polystyrene microspheres with soft poly(N-isopropylacrylamide) microgels and found that the microspheres self-assembled into anisotropic chains and phases with square symmetry at the air/water interface.<sup>53</sup> We attributed this non-intuitive phase behavior to the presence of a soft repulsion potential with a near-linear ramp profile interacting between the microspheres. The phase behavior was fully recovered by minimum energy calculations and Monte Carlo simulations using similar shapes of the interaction potential. We rationalized this interaction potential by assuming the formation of a two-dimensional, compressible microgel corona around the polymer microspheres in situ at the air/water interface. Accumulation repulsion<sup>54</sup> and elastic compressibility of this corona induce an effective repulsion of the microspheres, which may account for the postulated interaction potential. However, the system requires the microgel particles to be much smaller than the colloidal particles forming the anisotropic lattice, therefore limiting the observable structures to micron-sized particles.

Here, we aim to manipulate the interaction potential of smaller colloidal particles with sizes in the nanometer range by adopting a similar strategy. We hypothesize that other surface-active species may be similarly effective in manipulating the interaction potential between colloidal particles at the air/water interface, allowing the formation of complex assembly phases using isotropic, nanoscale colloidal particles.

We therefore investigate the assembly behavior of polystyrene (PS) colloidal particles in the presence of different types of molecular amphiphiles at the air/water interface, including classical surfactants, block copolymers and proteins. We characterize the self-assembly in situ by optical microscopy as well as after transfer to a solid substrate by scanning electron microscopy (SEM). For certain types of surfactants, we observe complex assembly phases, including chains and square lattices. We discuss criteria for the amphiphiles that are required to induce complex self-assembly structures and show that the observed structures agree with theoretical minimum energy calculations of hard spheres interacting via a soft-repulsion (Jagla) potential.

## Results

We used surfactant-free emulsion polymerization to synthesize polystyrene (PS) colloidal particles with acrylic acid as comonomer and ensured that the colloidal dispersions were free of impurities by applying dialysis and centrifugation. As amphiphilic additives, we investigated commercially available surfactants (Triton X-100, sodium dodecyl sulfate (SDS)), low molecular weight ionic block copolymers (BCP) poly(acrylic acid)-*block*-poly(methyl methacrylate) (poly(AA<sub>15</sub>-*block*-MMA<sub>15</sub>))<sup>55</sup> and the surface active protein bovine serum albumin (BSA). We premixed the colloidal dispersions with defined concentrations of an amphiphile, diluted the dispersions with 50 vol-% ethanol and spread them to the air/water interface of a Langmuir trough (Figure 1). To visualize the assembly as a function of the surface pressure (or, the particle density) we used two techniques: For small colloidal particles ( $d = 600$  nm), we used the simultaneous compression and deposition method to transfer the interfacial monolayer onto a solid substrate while compressing (Figure 1). This procedure enables us to transfer the full phase diagram onto a single substrate, which can then be imaged by SEM.<sup>56-58</sup> For large colloidal particles ( $d = 1.1$   $\mu\text{m}$ ) we directly visualized the assembly in situ by mounting the Langmuir trough set-up on top of a conventional optical microscope equipped with a camera.

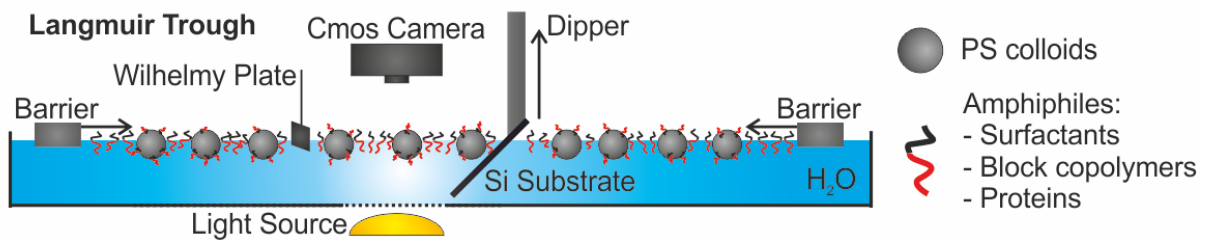


Figure 1: Interfacial behavior of colloidal particles at the air/water interface in the presence of amphiphiles: Schematic illustration of the experimental setup. Polystyrene colloidal particles ( $d = 600$  nm and  $d = 1.1$   $\mu$ m) are mixed with different concentrations of amphiphiles and spread onto the air/water interface of a Langmuir trough. The interfacial self-assembly was observed in situ by light microscopy or ex situ by deposition onto a solid substrate while simultaneously compressing the interface.

We first investigated the self-assembly of the PS colloidal particles in the presence of commercially available surfactants. We chose sodium dodecyl sulfate as a typical ionic surfactant with the same charge as the colloidal particles and Triton X-100 as non-ionic surfactant (Figure 2). The surface pressure – normalized area isotherm of a pure colloidal dispersion did not show any increase in surface pressure until all particles are in close contact, upon which the surface pressure increases very steeply (Figure 2a, black dashed line), in agreement with previous work.<sup>59–61</sup> For better comparison, all compression isotherms were normalized to the steep increase in surface pressure upon contact of the colloids ( $P = 40$  mN/m), which was defined as 1. We spread Triton X-100 at the air/water interface and compressed with two different velocities. Fast compression speeds (barrier speed = 10 mm/min, Figure 2a, red line) lead to a steady increase in surface pressure. Upon slow compression (barrier speed = 1 mm/min, Figure 2a, orange dotted line), the surface pressure remained nearly constant, indicating that the surfactant could desorb from the interface to maintain equilibrium. The isotherm of the mixed colloid particles/Triton X-100 system (Figure 2a, blue) can be

described by a superposition of the isotherms of the individual components. On the Langmuir trough (Figure 2b) we noticed a macroscopic phase separation into a hexagonal close packed colloid phase (Figure 2c) and a colloid-free, Triton X-100 phase, indicated by the orange circle in the photograph of Figure 2b. The surface pressure – normalized area isotherm of pure SDS spread at the air/water interface (Figure 2d) showed a similar dependence on the compression speed. With high compression speed (barrier speed = 10 mm/min, Figure 2d, red line) an increase in surface pressure was detected. At low compression speed (barrier speed = 1 mm/min, Figure 2d, orange dotted line), no increase in surface pressure was detected upon compression, indicating that the equilibrium surface tension is independent of the available surface. SDS therefore behaves as model water-soluble surfactant that desorbs into the water phase upon decrease in available surface area to maintain its equilibrium concentration at the interface.<sup>62</sup> Similarly, the compression speed had an influence on the mixed system. For fast compression, we observed a phase separated structure consisting of colloid-free areas surrounded in a matrix of hexagonal-close packed colloids (Figure 2e). With slow compression, SDS desorbed from the air/water interface, leading to an ordered hexagonal close packed colloidal monolayer at the interface (Figure 2f). We further tested the effect of adding SDS via the bulk phase ( $c(\text{SDS}) = 1 \text{ mmol/L}$ ) on the colloid assembly. After equilibration and by slow compression the colloids ordered into a hexagonal pattern, indicating that the addition method of SDS did not affect the phase behavior.

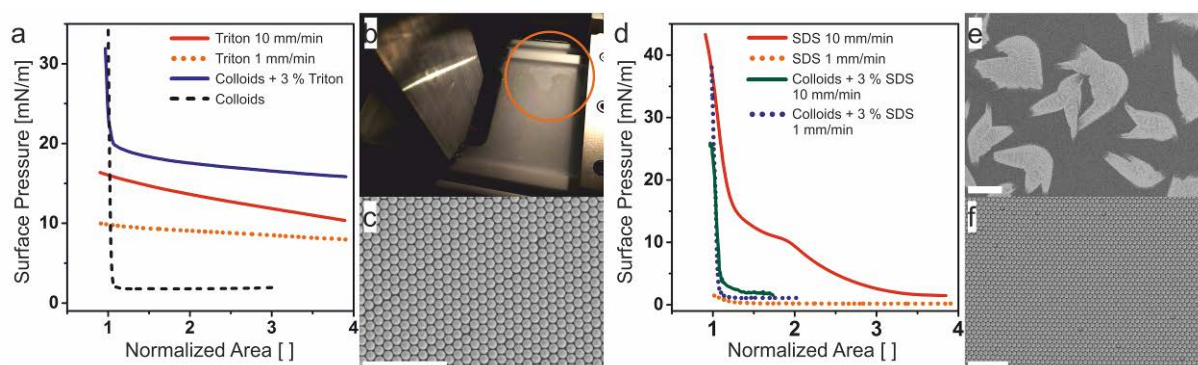


Figure 2: Co-assembly of negatively charged PS colloids ( $d = 600$  nm) with typical commercial surfactants. a) Surface pressure - normalized area isotherms of Triton X-100 and mixtures with colloidal particles. b,c) Co-assembly of PS colloids with Triton X-100. We observed a macroscopic phase separation on the Langmuir trough (b) even at high surface pressures ( $\pi > 25$  mN/m) into a hexagonal, well-ordered colloidal monolayer (c) and a colloid-free Triton X-100 region indicated by the orange circle (b). Scale bar:  $5 \mu\text{m}$ . d) Surface pressure - normalized area isotherms of sodium dodecyl sulfate (SDS) and mixtures with colloidal particles, indicating differences between kinetically controlled behavior (fast compression) and equilibrium behavior (slow compression). Mixtures of colloids with SDS showed a holey structure at high compression speed (e) (black area are hexagonally-packed colloids, white area colloid-free regions, scale bar:  $200 \mu\text{m}$ ) and a uniform hexagonal assembly at low compression speed (f). Scale bar:  $5 \mu\text{m}$ .

Next, we used the amphiphilic block copolymer (BCP) (poly(AA<sub>15</sub>-*block*-MMA<sub>15</sub>)). In its chemical composition, this block copolymer resembles the polymer colloids, which were synthesized using acrylic acid as the comonomer as well. At pH 7 the acrylic acid groups ( $\text{pK}_a = 4.25$ )<sup>63</sup> of the BCP are deprotonated and thus hydrophilic, while the MMA part remains hydrophobic, resulting in an amphiphilic behavior. The surface pressure – area isotherm of pure BCP shows a reduction in surface tension with decreasing interfacial area independent of the compression speed (Figure 3a, blue line and dotted blue line), indicating irreversible adsorption of the block copolymer at the interface. The interfacial behavior of polystyrene colloidal particles was affected by the presence of BCP. The surface pressure –area isotherms of mixed colloid/BCP systems, shown in Figure 3a, changed even with small BCP concentrations (Figure 3a). The isotherm of the mixed system showed an increase in surface pressure already at larger interfacial areas and a high compressibility of the interfacial layer, meaning that upon

reduction of the interface, the amphiphilic species changes the area it occupies at the interface.

With increasing BCP concentration, this behavior became more pronounced, indicating that the interfacial properties were increasingly dominated by the BCP (Figure 3a, brown to green lines).

In contrast to the case of the commercial surfactants shown above, the BCP induced changes in the self-assembly behavior of the colloidal particles at the interface. Figure 3b-e shows representative SEM images of the interfacial assembly transferred to a solid substrate at high surface pressures in the steep part of the isotherm ( $\Pi > 30\text{mN/m}$ ) where the interfacial layer was compressed to the maximum (even higher pressures led to buckling of the layer). As expected, pure PS colloids showed a hexagonal close packed lattice (Figure 3b). The composite system with BCP and colloids showed more complex phases. At the lowest BCP concentration of 0.05 wt%, we observed a lattice with distorted square packing (Figure 3c). Typical sizes of regions with square arrangements were rather small, which we tentatively attribute to capillary deformations during transfer. With increasing BCP concentrations, the colloidal particles assembled into anisotropic chains (0.07-0.2 wt%), which became shorter and more separated with increasing BCP concentration (Figure 3d-f). At the highest BCP concentration of 0.3 wt%, all colloidal particles were spatially separated and appeared disordered (Figure 3g). Due to irreversible adsorption of the BCP, the interface was predominantly covered with the BCP, preventing the colloidal particles from coming into closer contact.

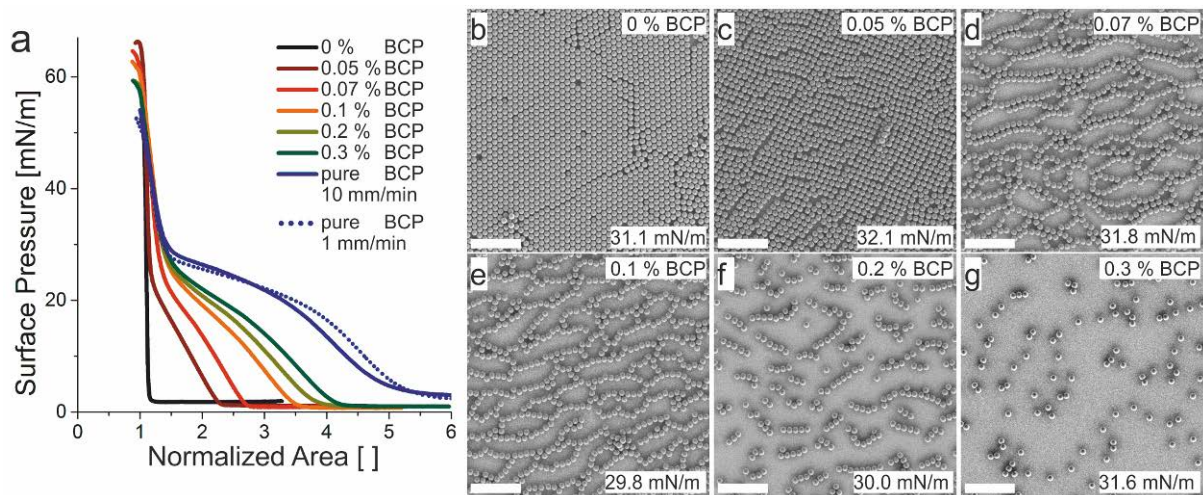


Figure 3: Coassembly of PS colloids ( $d = 600$  nm) with various poly(AA<sub>15</sub>-MMA<sub>15</sub>) block copolymers (BCP)<sup>55</sup> concentrations. a) Normalized compression isotherm: We noticed a smoother increase with increasing BCP/PS colloids mass ratio. b-g) Representative SEM images of the observed phases after transfer to a solid substrate: b) hexagonal close packed phase; c) square phase; d,e) chain phase; f) significantly shortened chains; h) separated particles. Scale bar: 5  $\mu$ m.

To understand the evolution of the complex interfacial arrangements of the BCP/colloid system in more detail, we investigated the phase behavior of the colloidal particles in the square- and chain region as a function of the surface pressure. Figure 4 shows the isotherm of the 0.05 wt% BCP/colloid mixture along with SEM images taken at different stages of the compression after transfer to a solid substrate. At lower pressures before the steep part of the isotherm ( $\Pi = 11.5$  mN/m; Figure 4b), we observe a coexistence of square and hexagonal packing, but visible cracks and local formation of close-packed structures indicates that capillary forces may have distorted the structure during drying. Direct observations of particles at the interface (Figure 6) confirm this distortion and show that at low surface pressure the particles at the interface arrange in disordered, non-close packed structures. At higher surface pressures in the steep part of the isotherm, we observed pseudo square arrangements over a

relative wide range of surface pressures, indicating that there is little rearrangement of the colloidal particles at high compressions after transfer to the solid substrate (Figure 4c-g). However, small deformations occurring upon drying by capillary forces may cause the relatively small crystal sizes. As we cannot exclude artifacts from the drying process, we refrained from a quantitative analysis of the phase behavior. Qualitatively, all observed phases can be directly correlated to the phase behavior directly at the interface (see below), indicating that capillary forces do not dominate the structure formation process. The measured high surface pressure values have to be taken with care, as extra and deviatoric stresses can occur.<sup>64</sup>

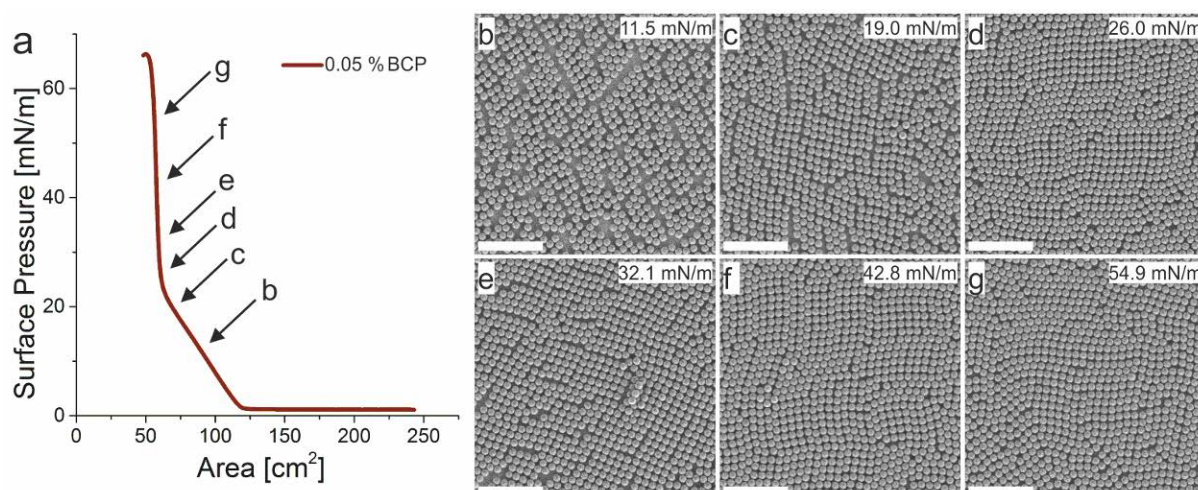


Figure 4: Phase diagram of a mixture of PS colloids ( $d = 600$  nm) and 0.05 wt% block copolymer (BCP). a) Surface pressure – area isotherm. b-g) Representative SEM images of the interfacial arrangement after transfer to a solid substrate. At low surface pressure (b,c), clustering of the particles indicates a disturbed arrangement caused by capillary forces upon drying. At high surface pressures, in the steep part of the isotherm ( $\Pi > 25$  mN/m) distorted square lattices of the colloidal particles were observed on the solid substrate (d-g). Scale bar: 5  $\mu$ m.

Figure 5 shows the surface pressure – area isotherm for the 0.1 wt% BCP/colloid system along with the transferred assembly structures. Similar to before, at lower surface pressures ( $\Pi < \sim 25$  mN/m), the transferred colloidal structures appear inhomogeneous and partially agglomerated, which we attribute to capillary forces acting upon drying (Figure 5b,c). In the steep part of the isotherm ( $\Pi > \sim 25$  mN/m), clear anisotropic chain phases are observed after transfer to a solid substrate. The chains seem to be preferentially arranged perpendicular to the barriers of the Langmuir trough, parallel to the direction of compression (Figure 5d-g).

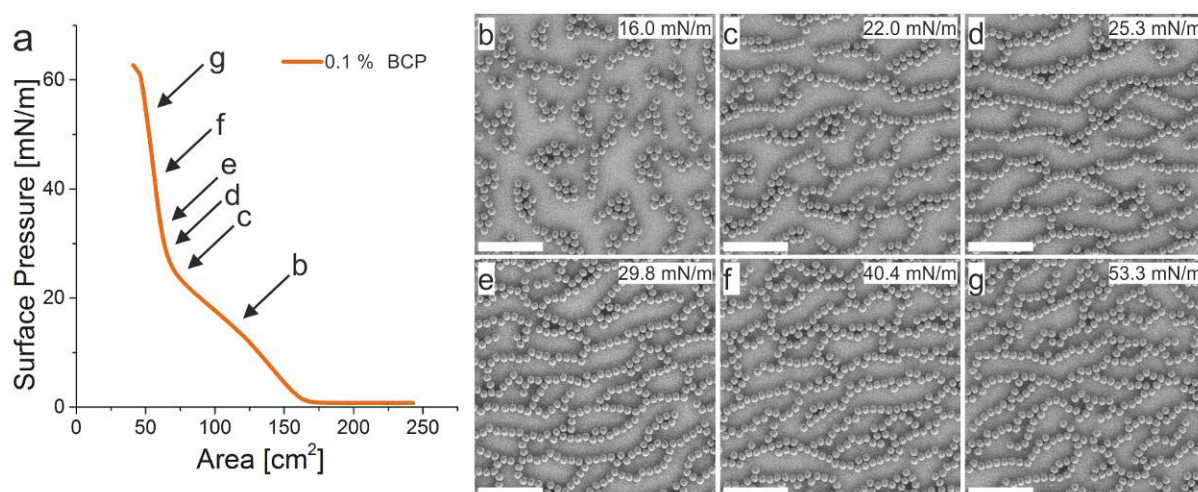


Figure 5: Phase diagram of a mixture of PS colloids ( $d = 600$  nm) and 0.1 wt% block copolymer (BCP) leading to a chain network phase. a) Surface pressure – area isotherm. b-g) Representative SEM images of the deposited structures after transfer to a solid substrate. At low surface pressures (b,c) irregular, partially clustered structures resulted presumably from capillary forces upon drying. At high surface pressures, in the steep part of the isotherm ( $\Pi > 25$  mN/m) anisotropic, chain structures are clearly visible (d-g). The chains seemed preferentially oriented perpendicular to the barriers of the Langmuir trough, parallel to direction of the compression. Scale bar: 5  $\mu$ m.

The small size of the colloidal particles prevents the direct observation of the structure of the monolayer formed at the air/water interface, requiring the indirect method of transferring the interfacial arrangement to a solid substrate to characterize the structure of the assembly by electron microscopy. This procedure, however, bears the risk that the structural arrangement is affected by capillary forces during the drying process. Indeed, images of the particle arrangements taken at lower transfer pressures show close packed structures and partial aggregation, which may have been caused by capillary forces (Figure 4b, Figure 5b). We increased the size of the colloidal particles ( $d = 1.1 \mu\text{m}$ ) and integrated the Langmuir trough into a microscope setup to directly observe the interfacial arrangement by optical microscopy.<sup>53</sup> Figure 6 shows the interfacial assembly phases of these large polystyrene microspheres at the air/water interface in the presence of BCP molecules. We observed a similar surface pressure – area isotherm as for the smaller particles, albeit with the change in slope shifted to a higher surface pressure (Figure 6a). The interfacial assembly of pure microspheres showed hexagonal close packed structures (Figure 6b). In the presence of the BCP, the interfacial assembly of the microspheres was more complex and transitioned from non-close packed arrangements at low surface pressure (Figure 6c) to anisotropic chain phases at higher surface pressures (Figure 6de). These results coincide with the assembly phases observed for the smaller colloids by electron microscopy, demonstrating that the interfacial assembly can be transferred to a solid substrate without altering its structure if the transfer is performed at high compression. At lower surface pressure, we observed non-close packed arrangements and chain structures at the interface, while the electron microscopy images showed close packed aggregates. We therefore conclude that ex-situ SEM imaging cannot be used to interpret the interfacial behavior at low surface pressures as capillary forces alter the structure of the assembly. It is noteworthy that the observed particle chains were preferentially aligned perpendicular to the barriers, similar to the case of smaller colloids investigated by SEM. The comparison of in-situ microscopy and electron microscopy underlines that it is possible to transfer the complex assembly phases to a

solid substrate, opening up avenues to create complex assembly structure for the nanostructuring of surfaces.

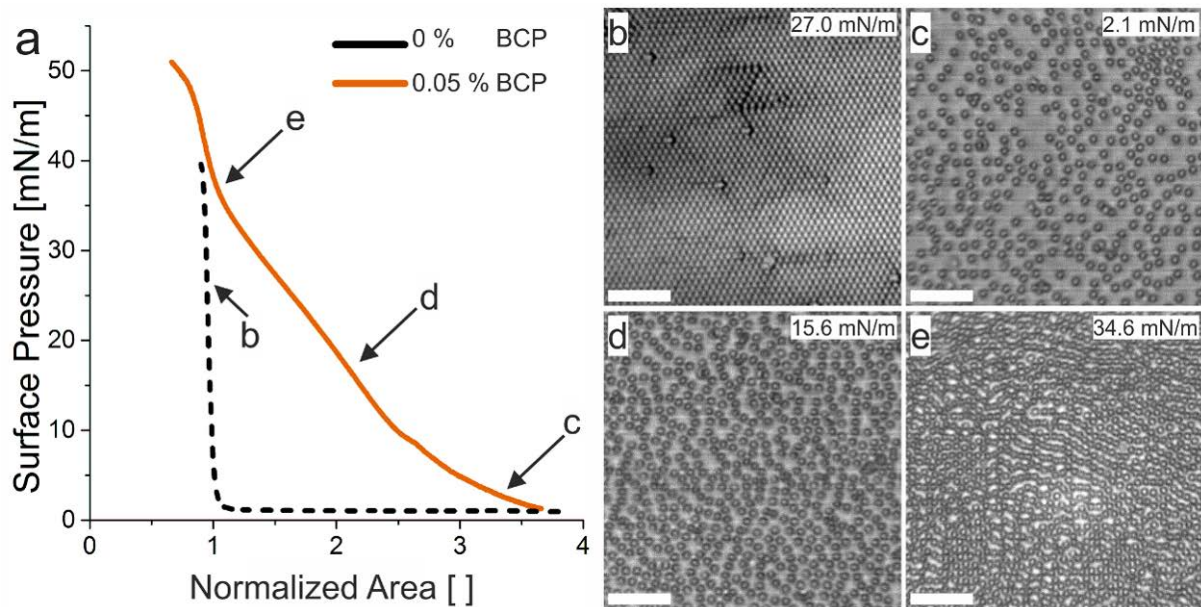


Figure 6: Direct observation of the interfacial arrangement of larger PS colloids ( $d = 1.1 \mu\text{m}$ ) in the presence of block copolymer (BCP). a) Normalized surface pressure – area isotherm of pure PS colloids (black dotted line) and PS colloids mixed with BCP (mass ratio colloids/BCP = 0.05 wt%) (orange). b) Microscopy image of pure PS colloids and mixed with BCP (c-e) at the air/water interface. In the presence of BCP the PS microspheres form chains instead of the expected hexagonal packing. Scale bar:  $10 \mu\text{m}$ .

Finally, we investigated the self-assembly of PS colloids in the presence of bovine serum albumin (BSA) (Figure 7). BSA is a well-studied surface-active model protein, showing a rigid, solid-like behavior when adsorbed at the air/water interface.<sup>65</sup> Fast and slow compression of pure BSA led to a similar surface pressure – area isotherm, indicating irreversible adsorption of BSA to the air/water interface, in agreement with reports in literature.<sup>66,67</sup> The presence of BSA induced similar changes in the surface pressure – area isotherm as the BCP and showed

an increase in surface pressure at lower compressions compared to the pure colloidal particles. This increase in surface pressure became more pronounced with increasing concentration of BSA (Figure 7a). With increasing protein concentration the structure of the transferred monolayer shifted from hexagonal close packing (0 wt% BSA, Figure 7b) to a square-like arrangement coexisting with hexagonal regions (1.5 wt% BSA; Figure 7c), to anisotropic chains (2 wt% BSA; Figure 7d), to isolated colloidal particles (3 wt% BSA; Figure 7e).

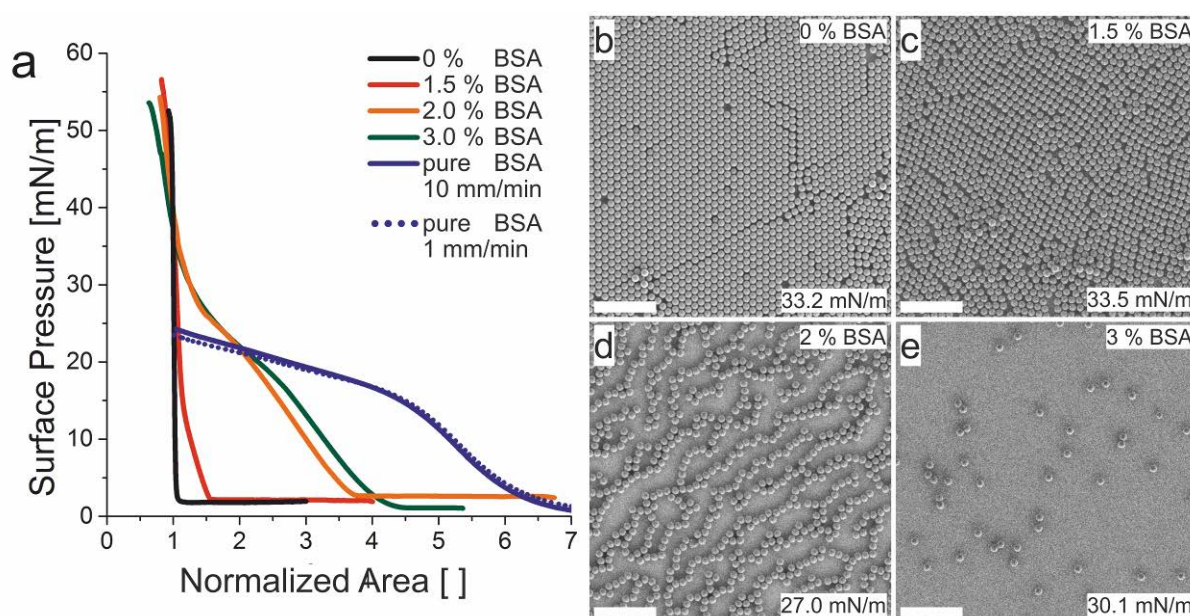


Figure 7: Phase diagram of a mixture of colloids ( $d = 600$  nm) with bovine serum albumin (BSA): a) Normalized compression isotherms for different concentrations of BSA. b-e) Representative images of the different phases observed: b) hexagonal close packed phase, c) square phase, d) chain phase, f) single colloids. Scale bar:  $5 \mu\text{m}$ .

## Discussion

Our experiments indicate that some molecular additives present at the air/water interface alter the self-assembly of colloidal particles at the air/water interface. These amphiphiles direct the colloidal particles into pseudo-square or chain phases, which is not expected for isotropic, spherical colloidal particles.

We discuss this complex phase behavior in the context of a change in the interaction potential acting between the colloidal particles. Previously, we demonstrated that polystyrene microspheres in the presence of soft microgels showed a similar phase behavior and underwent phase transitions upon compression from a non-close packed phase, to a chain phase, to a pseudo-square phase until finally forming a hexagonal close packed phase.<sup>53</sup> This phase behavior coincided with theoretical predictions based a long-range, linear repulsive contribution to the interaction potential between the microspheres. We rationalized this interaction potential by the in-situ formation of a two-dimensional corona of small particles around a large particle directly at the interface. This corona forms by adsorption of the microgels to the particles' surfaces and the presence of additional microgels surrounding this layer of adsorbed microgels. These microgels are forced to overlap upon decreasing the area available at the interface, which, in turn, creates a repulsive force as the polymer chains are forced into closer contact. The two-dimensional nature of this compressible shell translates into a linear increase in overlap area with decreasing distance between the microspheres – which we hypothesized to cause a linear increase in the repulsion, as required by the theoretical considerations to form the complex assembly phases.<sup>53</sup>

The close similarity to the phase behavior we observe for smaller colloidal particles in the presence of some of the amphiphiles leads to the assumption that these amphiphiles affect the interaction potential in a similar way as the microgels (as schematically illustrated in Figure 9).

In analogy to the case of microgels, we hypothesize that the repulsive component of the interaction potential is caused by an accumulation of amphiphiles in between the colloidal

particles at the air/water interface. In this picture, the amphiphiles adsorb to the particle surface and accumulate in between the particles, with the following consequences for the interaction potential. First, the accumulation of the amphiphiles itself causes an effective repulsion of the large particles, which are pushed apart from each other as amphiphiles accumulate in between the particles. This phenomenon is known as accumulation repulsion<sup>54</sup> and is directly observable from the microscopy investigations of the interfacial assemblies in Figure 6. In the presence of amphiphiles, the colloidal particles show a non-close packed arrangement at minimal compression, indicating a net repulsive character. Second, the two-dimensional layer of amphiphiles present in between the particles is forced into increasingly closer contact upon compression, which adds to the repulsive character of the system when we increase the overlap. From these considerations, we deduce the following requirements for the additive to be able to alter the phase behavior of the colloidal particles.

Surface activity. The additive must adsorb to the air/water interface to form a two-dimensional layer in between the colloidal particles. The two-dimensional nature of this shell surrounding the colloidal particles seems to be crucial to achieve the required (linear) shape of the interaction potential, since the area of overlap between the amphiphiles changes linearly upon compression in a two-dimensional layer.<sup>53</sup> This requirement seems trivial but is the reason why amphiphilic components need to be chosen as the additive to be co-assembled with the colloidal particles and why three-dimensional core-shell particles do not exhibit this behavior.<sup>53,56,68,69</sup>

Homogeneous co-assembly with the colloidal species. The hypothesized change in interaction potential relies on the formation of a homogeneous, two-dimensional corona of amphiphilic molecules around the colloidal particles (Figure 1). The formation of this homogeneous layer requires an affinity between the two species at the interface. Phase separation of amphiphile and colloids therefore needs to be prevented.

Irreversible adsorption. The amphiphile needs to adsorb strongly, almost irreversibly, to the air/water interface to enable compression without desorption into the subphase. The two-dimensional corona formed around the particles can only contribute to the complex phase behavior if the area per particle can be changed (i.e. by compression of the interface) without losing the corona by desorption from the interface.

Compressibility of the amphiphile layer. We hypothesize that the amphiphile corona needs to be compressible in order to generate a longer range repulsive shoulder between the particles, similar to the case of microgel additives.<sup>53</sup>

Next, we argue how these criteria relate to the different interfacial species and discuss why some of the tested species do influence the assembly behavior while others do not. First, we note that all species fulfil criterion 1, i.e. they are all surface active in the presence of the colloidal particles as can be seen from the changes in the surface pressure – area isotherms of all mixed samples. Second, we note that the commercial surfactant Triton X-100 does not induce any change in the phase behavior of the colloidal particles (Figure 2a-c), but instead causes a macroscopic phase separation. The surfactant does not form a corona around the colloids and thus does not fulfill criteria two. The other tested commercial surfactant SDS does desorb from the air/water interface. The interfacial surfactant layer is therefore removed upon compression, preventing the formation of an irreversible corona around the PS colloids, described in criteria three. For the other surface-active species (block copolymer (BCP), and protein) we did not observe any phase separation or desorption from the interface. Both species also induced a complex phase behavior, supporting the criteria put forward above.

In a proof of principle experiment, we performed the interfacial assembly of BCP and colloids on a subphase with a defined amount of salt. We hypothesized that salt will screen the charges of the acrylic acid groups in the block copolymer and therefore decrease the repulsion in the system, forming more compact polymer coils and therefore reduce the compressibility at the

interface. With increasing salt addition, we observed that the surface pressure – area isotherm became steeper and less compressible (Figure 8), as predicted for the more compact polymer chains. The phase behavior of the colloidal particles observed after transfer to a solid substrate changed significantly with increasing salt concentration and chain formation was only observed in the absence of salt (Figure 8b-d), indicating that compressibility, i.e. the ability to force the surfactant layer into closer overlap, is important to observe the complex assembly phases as well.

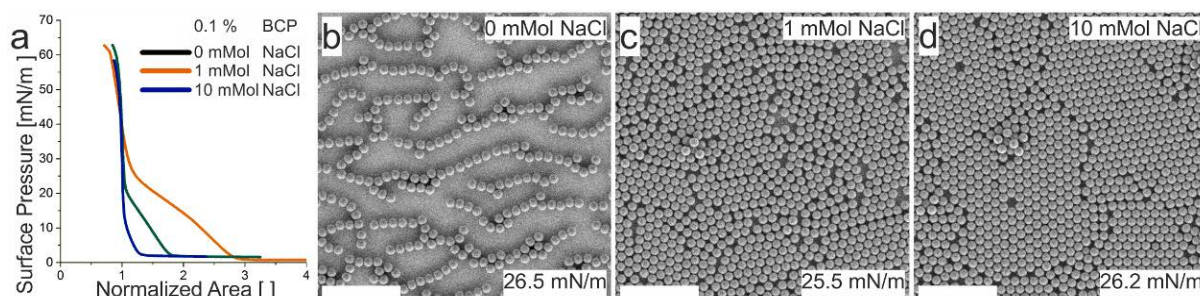


Figure 8: Effect of salt addition on the self-assembly of colloids ( $d=600$  nm) with block copolymer. a) normalized compression isotherm: ‘soft shoulder area’ decreases with more salt. b-d) Representative SEM image of transferred assembly on a silicon wafer. By the addition of NaCl salt the chain phase (b) shifts to hexagonal close packed phase with 1 mMol/L (c) and 10 mMol/L salt (d). Scale bar:  $5 \mu\text{m}$

Finally, we discuss the effect of amphiphile concentration on the resulting interfacial assembly properties that we experimentally observe (Figure 3). With increasing concentration of block copolymer, the assembly phases at maximum compression shift from pseudo square packing to anisotropic chains, which subsequently become shorter and more widely spaced, until, at maximum BCP concentration, only individual, separated particles are observed. We note that there is a significant scatter in colloidal chain lengths, chain orientation and inter-chain distance, which only allows a qualitative discussion of these effects.

Within the framework of our simple core-shell model, an increase in the amphiphile concentration will increase the range of the soft repulsive shoulder, as more and more amphiphiles separate the colloidal particles. The assumed interaction potential should therefore be controlled by the amphiphile concentration.

Previously, we showed that the core-shell model could reproduce the experimental phase behavior for the case where shell thickness was fixed while the surface pressure/colloid area fraction was increased.<sup>49</sup> Here, we show that the model can also reproduce the phase behavior observed in Figures 3 and 7, i.e., where the surface pressure is fixed, but the shell thickness is increased.

We model the interaction between the core-shell particles using the Jagla potential with a linear ramp profile for the soft shoulder (Figure 9a); this is equivalent to assuming that the soft shoulder profile parameter  $g = 1$ . In Figure 9a,  $r_0, r_1$  are the range of the hard core and soft shoulder respectively (or equivalently the diameter of the hard core and soft shell respectively), while  $U_0$  is the potential shoulder height. As detailed elsewhere,<sup>53</sup> the quantity  $U_0$  is the work required to fully overlap the soft shells of two core-shell particles and can be approximated as  $U_0 \approx P_0 A_{overlap}$  where  $P_0$  is the surface pressure of the amphiphile at the plateau of the surface pressure-area isotherm,  $A_{overlap} = \frac{r_1^2}{2} \left( \theta - \frac{r_0}{r_1} \sin \theta \right)$  is the overlap area between two fully overlapped shells and  $\theta = \cos^{-1} \left( \frac{r_0}{r_1} \right)$ . From Figure 3a, we determine  $P_0 \approx 30 \text{mN/m}$  for the BCP system while from Figure 7a,  $P_0 \approx 25 \text{mN/m}$  for the BSA protein system. Importantly,  $P_0$  approximately correlates to the surface pressure at which the different characteristic phases shown in Figures 3, 7 were observed.

We performed a comprehensive exploration of the minimum energy structures containing one particle per unit cell (Figure 9b) in the NPT ensemble. Specifically, we determined the minimum energy configuration (MEC) for a given value of  $r_1/r_0$  and  $P$  by minimizing the enthalpy per particle  $H$  with respect to the lattice parameters shown in Figure 9b. Note that the

MECs are relevant experimentally since in the experimental system  $U_0 \gg k_B T$  so that we are effectively in the zero temperature regime.

In Figure 9c, we sketch the minimum energy phase diagram for our theoretical core-shell particles in the  $r_1/r_0$  vs.  $P/P_0$  plane. The horizontal dashed line at  $P \approx P_0$  corresponds to the experimental conditions at the observed phases in Figures 3 and 7. As we increase  $r_1/r_0$  along this horizontal line (dotted line in Figure 9c, Figure 9d) the equilibrium structure changes from the high-density hexagonal phase (HEX-H), to rhomboids (RH), to rectangles (REC), to chains (CH) and finally to the low-density hexagonal phase (HEX-L).

Note that for the range of  $r_1/r_0$  values spanned by the RH and REC phase at  $P = P_0$ , both phases are close to the square phase (which has unit cell angle  $\phi = 90^\circ$  and unit cell aspect ratio  $\gamma = b/a = 1$ ). For example in Figure 9c, the unit cell angle for the RH phase ( $\gamma = 1$ ) ranges from  $\phi = 105^\circ$  (at point B) to  $\phi = 90^\circ$  (at point C). Similarly, the unit cell aspect ratio for the REC phase ( $\phi = 90^\circ$ ) ranges from  $\gamma = 1$  (at point C) to  $\gamma = 1.1$  (at point D). The sequence of phases predicted by our theoretical model along the dashed line in Figure 9c is therefore in excellent agreement with the experimental data in Figures 3 and 7, with the equilibrium structure evolving from high-density hexagons, to square-like structures, to chains to high-density hexagons with increasing  $r_1/r_0$ .

As a final detail, we note that preferential orientation of the colloidal chains perpendicular to the barriers that we observe in experiments can be rationalized from our hard core/soft shell model as well by taking into account the anisotropic compression of the interface (i.e. in the direction of the barrier movement). When we compress the core-shell particles so that their soft shells start to overlap, the anisotropy of the compressive field means that all the initial overlaps lie along the direction of the compression. The orientation of these initial overlaps breaks the symmetry of the system and biases the system to form fully overlapped shells along the direction of the compression in order to prevent the overlap of shells perpendicular to the

direction of compression. This process results in the formation of chains that are oriented parallel to the direction of compression.

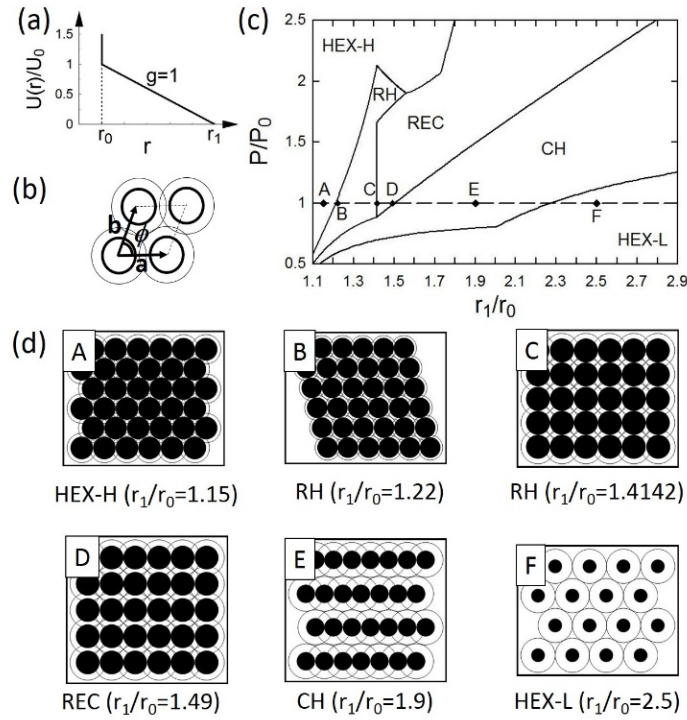


Figure 9: Minimum energy structures and phase behavior of particles with a soft repulsive shell. a) Jagla potential with linear ramp soft shoulder repulsion for the core-shell particles. b) Unit cell used in our calculations of two-dimensional structures, where  $\mathbf{a}$ ,  $\mathbf{b}$  are the lattice vectors,  $\phi$  is the unit cell angle and the thick and thin circles represent the particle core and corona, respectively. c) Zero temperature phase diagram in the  $r_1/r_0$  and reduced pressure  $P/P_0$  plane for particles interacting via the Jagla potential shown in a). The dashed line correspond  $P/P_0 = 1$  and represents the surface pressures used in to observe the experimental assembly phases. d) Representative minimum energy configurations at different points along the dashed line in c), where the capital letters in the insets refer to the state points labelled in c). The smaller filled circles and the larger open circles represent the particle core and corona, respectively.

## Conclusion

In this study, we observed that the presence of block copolymer or protein changes the assembly behavior of the colloids confined at an air/water interface.

While pure colloids assemble into a hexagonal close packed lattice, the observed colloidal phases transition from a distorted square lattice, via chain structures to fully separated colloidal particles with increasing amount of amphiphiles. We further investigated the assembly behavior of the colloid/BCP mixture in situ at the air/water interface, where we observed a chain assembly even at low surface pressures, thus excluding possible artefacts during the deposition of the interfacial assembly onto a solid substrate.

The observed structures are in agreement with minimum energy calculations based on isotropic particles interacting via a long-range repulsive shoulder known as Jagla potential. We hypothesize that the repulsive component of the interaction potential may be caused by an accumulation of amphiphiles in between the colloidal particles at the air/water interface, which cause an effective repulsion of the large colloidal particles by accumulation repulsion. The two-dimensional layer of amphiphiles around the colloids thus acts as soft corona separating the colloidal particles.

With increasing concentration of amphiphiles, this two-dimensional corona increases in size and therefore alters the phase behavior. The corona size - dependent phase behavior is reproduced by the theoretical model.

Our results provide an experimental simple pathway to direct the self-assembly of spherical colloids into complex anisotropic structures. This methodology opens pathways to increase the structural variety of nanoscale surface patterns created by colloidal lithography.

## Methods:

Materials: Acrylic acid (Sigma Aldrich, 99 %), ammonium persulfate (APS, Sigma Aldrich, 98 %), sodium dodecyl sulfate (SDS, Sigma Aldrich, 98 %), ethanol (EtOH, Sigma Aldrich, 99.9 %), Trinton X-100<sup>TM</sup>), sodium hydroxide (NaOH, Carl Roth, 99 %), sodium chloride (NaCl, Sigma Aldrich, 99.5 %) were used as received.

Styrene (Sigma Aldrich, 99 %) was purified by adding a 10 wt-% NaOH solution in a volume ratio 1:1. After vigorous shaking, the aqueous was discarded and the styrene phase passed through an aluminum oxide powder column. The water used was double deionized using a Milli-Q system with a resistivity of 18 M $\Omega$ .

Synthesis: Synthesis of polystyrene microspheres: Polystyrene (PS) microspheres were synthesized by a surfactant-free emulsion polymerization. In short, 250 mL Milli-Q water was heated to 80 °C in a 500 mL triple-neck round-bottom flask with reflux-condenser and degassed by bubbling with nitrogen gas for 30 min. 40 g styrene were added to the water phase under constant stirring. 0.2 g of the comonomer acrylic acid was dissolved in 5 mL Milli-Q water and added to the mixture. After 5 min the reaction was initiated with 0.1 g ammonium persulfate, dissolved in 5 mL Milli-Q water. The reaction was carried out for one day at 80 °C. After cooling to room temperature, the dispersion was filtered and purified by centrifugation and redispersion and applying dialysis against water for 2 months.

The detailed synthesis for the low molecular weight ionic block copolymers (BCP, Poly(AA<sub>15</sub>-*block*-MMA<sub>15</sub>)) is described in a previous publication.<sup>55</sup> In short, BCP were synthesized by sequential living anionic polymerization of tert-butyl acrylate and methyl methacrylate initiated by (diphenylhexyl)lithium in the presence of lithium chloride. The tert-butyl esters of the polymer were hydrolyzed with HCl. The BCP were dissolved in Milli-Q water under basic conditions using 0.1 M NaOH to a concentration of 0.1 wt%.

Langmuir trough: Prior to the experiment, the PS colloids ( $d = 600$  nm) were cleaned 3 times by centrifugation and redispersion to avoid any possible contamination. The suspension was diluted to 1 wt% with Milli-Q water and ethanol in a ratio 1:1. The respective amount of amphiphile was added and mixed in an ultrasound bath for 5 min. For the simultaneous compression and deposition we used a Teflon® Langmuir trough (KSVNIMA) with an area of 243 cm<sup>2</sup> and a width of 7.5 cm. The barriers are made of Delrin® and the surface pressure is measured by a Wilhelmy plate. Silicon wafers (Siltronix®) were cut to 8 x 1 cm<sup>2</sup> and cleaned by ultrasonication in ethanol and Milli-Q water, followed by oxygen plasma (Diener). The substrate was mounted to a substrate holder in a 45° angle and lowered into the Milli-Q water filled trough. The mixed amphiphile/colloid suspension was spread at the air/water interface and equilibrated for 30 min. The barriers were compressed by 4 mm/min and the dipper was elevated at 0.8 mm/min. The deposited assembly was further characterized by SEM. Further we investigated the effect of compression speed under fast (barrier speed = 10 mm/min) and slow (barrier speed = 1 mm/min) compression. To compare the effect of amphiphiles on the shape of the compression isotherm we normalized the area to the steep increase in surface pressure upon contact of the colloids ( $P = 40$  mN/m), which was defined as 1.

For in-situ observation of the particle assembly at the air/water interface we mounted the Langmuir trough set-up on an optical microscope (Leitz, Ergolutz) equipped with a CMOS camera (Thorlabs, DCC1645C). We used larger PS colloids ( $d = 1.1$  μm) and a high compression trough with a glass window in the center and an area of 550 cm<sup>2</sup>. The images were taken as 8-bit-grey-scale images in transmission mode with a 50x objective (Leitz Wetzlar). The barriers were compressed with a speed of 4 mm/min.

## AUTHOR INFORMATION

### Corresponding author

\* Email: nicolas.vogel@fau.de

### Author Contributions

‡ These authors contributed equally

### Founding Sources

The research was supported by the Deutsche Forschungsgemeinschaft (DFG) under grant number VO 1824/6-1. M.R., T.Y., K.B., and N.V. also acknowledge support by the Interdisciplinary Center for Functional Particle Systems (FPS) at Friedrich-Alexander University Erlangen-Nürnberg.

### References

- (1) Grzelczak, M.; Vermant, J.; Furst, E. M.; Liz-Marzán, L. M. Directed Self-Assembly of Nanoparticles. *ACS Nano* **2010**, *4*, 3591–3605.
- (2) Manoharan, V. N. Colloidal Matter: Packing, Geometry, and Entropy. *Science* **2015**, *349*, 1253751–1253751.
- (3) Vogel, N.; Retsch, M.; Fustin, C. A.; Del Campo, A.; Jonas, U. Advances in Colloidal Assembly: The Design of Structure and Hierarchy in Two and Three Dimensions. *Chem. Rev.* **2015**, *115*, 6265–6311.
- (4) Van Blaaderen, A. Materials Science: Colloids Get Complex. *Nature* **2006**, *439*, 545–

546.

- (5) Zhang, J.; Li, Y.; Zhang, X.; Yang, B. Colloidal Self-Assembly Meets Nanofabrication: From Two-Dimensional Colloidal Crystals to Nanostructure Arrays. *Adv. Mater.* **2010**, *22*, 4249–4269.
- (6) Velev, O. D.; Gupta, S. Materials Fabricated by Micro- and Nanoparticle Assembly - The Challenging Path from Science to Engineering. *Adv. Mater.* **2009**, *21*, 1897–1905.
- (7) Phillips, K. R.; England, G. T.; Sunny, S.; Shirman, E.; Shirman, T.; Vogel, N.; Aizenberg, J. A Colloidoscope of Colloid-Based Porous Materials and Their Uses. *Chem. Soc. Rev.* **2016**, *45*, 281–322.
- (8) Pieranski, P. Two-Dimensional Interfacial Colloidal Crystals. *Phys. Rev. Lett.* **1980**, *45*, 569–572.
- (9) Vogel, N.; Weiss, C. K.; Landfester, K. From Soft to Hard: The Generation of Functional and Complex Colloidal Monolayers for Nanolithography. *Soft Matter* **2012**, *8*, 4044.
- (10) Stamou, D.; Duschl, C.; Johannsmann, D. Long-Range Attraction between Colloidal Spheres at the Air-Water Interface: The Consequence of an Irregular Meniscus. *Phys. Rev. E - Stat. Physics, Plasmas, Fluids, Relat. Interdiscip. Top.* **2000**, *62*, 5263–5272.
- (11) Aveyard, R.; Clint, J. H.; Nees, D.; Paunov, V. N. Compression and Structure of Monolayers of Charged Latex Particles at Air / Water and Octane / Water Interfaces. *Langmuir* **2000**, *16*, 1969–1979.
- (12) Rey, M.; Elnathan, R.; Ditcovski, R.; Geisel, K.; Zanini, M.; Fernandez-Rodriguez, M. A.; Naik, V. V.; Frutiger, A.; Richtering, W.; Ellenbogen, T.; *et al.* Fully Tunable Silicon Nanowire Arrays Fabricated by Soft Nanoparticle Templating. *Nano Lett.* **2016**,

- 16, 157–163.
- (13) Kolle, M.; Salgard-Cunha, P. M.; Scherer, M. R. J.; Huang, F.; Vukusic, P.; Mahajan, S.; Baumberg, J. J.; Steiner, U. Mimicking the Colourful Wing Scale Structure of the *Papilio Blumei* Butterfly. *Nat Nano* **2010**, *5*, 511–515.
- (14) Nemiroski, A.; Gonidec, M.; Fox, J. M.; Jean-Remy, P.; Turnage, E.; Whitesides, G. M. Engineering Shadows to Fabricate Optical Metasurfaces. *ACS Nano* **2014**, *8*, 11061–11070.
- (15) Volk, K.; Fitzgerald, J. P. S.; Ruckdeschel, P.; Retsch, M.; König, T. A. F.; Karg, M. Reversible Tuning of Visible Wavelength Surface Lattice Resonances in Self-Assembled Hybrid Monolayers. *Adv. Opt. Mater.* **2017**, *5*.
- (16) Boechler, N.; Eliason, J. K.; Kumar, A.; Maznev, A. A.; Nelson, K. A.; Fang, N. Interaction of a Contact Resonance of Microspheres with Surface Acoustic Waves. *Phys. Rev. Lett.* **2013**, *111*, 1–5.
- (17) Khanolkar, A.; Wallen, S.; Abi Ghanem, M.; Jenks, J.; Vogel, N.; Boechler, N. A Self-Assembled Metamaterial for Lamb Waves. *Appl. Phys. Lett.* **2015**, *107*, 71903.
- (18) Stelling, C.; Singh, C. R.; Karg, M.; König, T. A. F.; Thelakkat, M.; Retsch, M. Plasmonic Nanomeshes: Their Ambivalent Role as Transparent Electrodes in Organic Solar Cells. *Sci. Rep.* **2017**, *7*, 1–13.
- (19) Bley, K.; Semmler, J.; Rey, M.; Zhao, C.; Martic, N.; Klupp Taylor, R. N.; Stingl, M.; Vogel, N. Hierarchical Design of Metal Micro/Nanohole Array Films Optimizes Transparency and Haze Factor. *Adv. Funct. Mater.* **2018**, *1706965*, 1706965.
- (20) Tsai, H. J.; Lee, Y. L. Facile Method to Fabricate Raspberry-like Particulate Films for Superhydrophobic Surfaces. *Langmuir* **2007**, *23*, 12687–12692.

- (21) Utech, S.; Bley, K.; Aizenberg, J.; Vogel, N. Tailoring Re-Entrant Geometry in Inverse Colloidal Monolayers to Control Surface Wettability. *J. Mater. Chem. A* **2016**, *4*, 6853–6859.
- (22) Cremmel, C. V. M.; Zink, C.; Maniura-Weber, K.; Isa, L.; Spencer, N. D. Orthogonal Morphological Feature Size and Density Gradients for Exploring Synergistic Effects in Biology. *Langmuir* **2015**, *31*, 8446–8452.
- (23) Elnathan, R.; Delalat, B.; Brodoceanu, D.; Alhmoud, H.; Harding, F. J.; Buehler, K.; Nelson, A.; Isa, L.; Kraus, T.; Voelcker, N. H. Maximizing Transfection Efficiency of Vertically Aligned Silicon Nanowire Arrays. *Adv. Funct. Mater.* **2015**, *25*, 7215–7225.
- (24) Lee, Y. H.; Shi, W.; Lee, H. K.; Jiang, R.; Phang, I. Y.; Cui, Y.; Isa, L.; Yang, Y.; Wang, J.; Li, S.; *et al.* Nanoscale Surface Chemistry Directs the Tunable Assembly of Silver Octahedra into Three Two-Dimensional Plasmonic Superlattices. *Nat. Commun.* **2015**, *6*, 6990.
- (25) Geuchies, J. J.; van Overbeek, C.; Evers, W. H.; Goris, B.; de Backer, A.; Gantapara, A. P.; Rabouw, F. T.; Hilhorst, J.; Peters, J. L.; Konovalov, O.; *et al.* In Situ Study of the Formation Mechanism of Two-Dimensional Superlattices from PbSe Nanocrystals. *Nat. Mater.* **2016**, *15*, 1248.
- (26) Bianchi, E.; Capone, B.; Coluzza, I.; Rovigatti, L.; van Oostrum, P. D. J. Limiting the Valence: Advancements and New Perspectives on Patchy Colloids, Soft Functionalized Nanoparticles and Biomolecules. *Phys. Chem. Chem. Phys.* **2017**, *19*, 19847–19868.
- (27) Chen, Q.; Bae, S. C.; Granick, S. Directed Self-Assembly of a Colloidal Kagome Lattice. *Nature* **2011**, *469*, 381–384.
- (28) Gangwal, S.; Pawar, A.; Kretzschmar, I.; Velev, O. D. Programmed Assembly of

- Metallo-dielectric Patchy Particles in External AC Electric Fields. *Soft Matter* **2010**, *6*, 1413.
- (29) Leunissen, M. E.; Vutukuri, H. R.; Van Blaaderen, A. Directing Colloidal Self-Assembly with Biaxial Electric Fields. *Adv. Mater.* **2009**, *21*, 3116–3120.
- (30) Gong, T.; Wu, D. T.; Marr, D. W. M. Two-Dimensional Electrohydrodynamically Induced Colloidal Phases. *Langmuir* **2002**, *18*, 10064–10067.
- (31) Yang, Y.; Gao, L.; Lopez, G. P.; Yellen, B. B. Tunable Assembly of Colloidal Crystal Alloys Using Magnetic Nanoparticle Fluids. *ACS Nano* **2013**, *7*, 2705–2716.
- (32) Froltsov, V. A.; Blaak, R.; Chremos, A.; Likos, C. N.; Loewen, H. Crystal Structures of Two-Dimensional Binary Mixtures of Dipolar Colloids in Tilted External Magnetic Fields. *J. Phys. Chem. B* **2009**, *113*, 12316–12325.
- (33) Osterman, N.; Babič, D.; Poberaj, I.; Dobnikar, J.; Zihlerl, P. Observation of Condensed Phases of Quasiplanar Core-Softened Colloids. *Phys. Rev. Lett.* **2007**, *99*, 1–4.
- (34) Cavallaro, M.; Botto, L.; Lewandowski, E. P.; Wang, M.; Stebe, K. J. From the Cover: Curvature-Driven Capillary Migration and Assembly of Rod-like Particles. *Proc. Natl. Acad. Sci.* **2011**, *108*, 20923–20928.
- (35) Davies, G. B.; Krüger, T.; Coveney, P. V.; Harting, J.; Bresme, F. Assembling Ellipsoidal Particles at Fluid Interfaces Using Switchable Dipolar Capillary Interactions. *Adv. Mater.* **2014**, *26*, 6715–6719.
- (36) Shindel, M. M.; Wang, S.-W.; Mohraz, A. Interfacial Polymer Phase Segregation and Self-Assembly of Square Colloidal Crystals. *Soft Matter* **2012**, *8*, 6684.
- (37) Ershov, D.; Sprakel, J.; Appel, J.; Cohen Stuart, M. a; van der Gucht, J. Capillarity-

- Induced Ordering of Spherical Colloids on an Interface with Anisotropic Curvature. *Proc. Natl. Acad. Sci. U. S. A.* **2013**, *110*, 9220–9224.
- (38) Koenig, G. M.; Lin, I.-H.; Abbott, N. L. Chemoresponsive Assemblies of Microparticles at Liquid Crystalline Interfaces. *Proc. Natl. Acad. Sci.* **2010**, *107*, 3998–4003.
- (39) Gharbi, M. A.; Nobili, M.; In, M.; Prévot, G.; Galatola, P.; Fournier, J. B.; Blanc, C. Behavior of Colloidal Particles at a Nematic Liquid Crystal Interface. *Soft Matter* **2011**, *7*, 1467–1471.
- (40) Xia, D.; Brueck, S. R. J. A Facile Approach to Directed Assembly of Patterns of Nanoparticles Using Interference Lithography and Spin Coating. *Nano Lett.* **2004**, *4*, 1295–1299.
- (41) Lu, C.; Möhwald, H.; Fery, A. A Lithography-Free Method for Directed Colloidal Crystal Assembly Based on Wrinkling. *Soft Matter* **2007**, *3*, 1530.
- (42) Pazos-Pérez, N.; Ni, W.; Schweikart, A.; Alvarez-Puebla, R. A.; Fery, A.; Liz-Marzán, L. M. Highly Uniform SERS Substrates Formed by Wrinkle-Confined Drying of Gold Colloids. *Chem. Sci.* **2010**, *1*, 174.
- (43) Jagla, E. A. Phase Behavior of a System of Particles with Core Collapse. *Phys. Rev. E* **1998**, *58*, 11.
- (44) Jagla, E. A. Minimum Energy Configurations of Repelling Particles in Two Dimensions. *J. Chem. Phys.* **1999**, *110*, 451–456.
- (45) Malescio, G.; Pellicane, G. Stripe Phases from Isotropic Repulsive Interactions. *Nat. Mater.* **2003**, *2*, 97–100.

- (46) Glaser, M. A.; Grason, G. M.; Kamien, R. D.; Košmrlj, A.; Santangelo, C. D.; Zihlerl, P. Soft Spheres Make More Mesophases. *Europhys. Lett.* **2007**, *78*, 46004.
- (47) Pattabhiraman, H.; Dijkstra, M. On the Formation of Stripe, Sigma, and Honeycomb Phases in a Core-Corona System. *Soft Matter* **2017**, *13*.
- (48) Dotera, T.; Oshiro, T.; Zihlerl, P. Mosaic Two-Lengthscale Quasicrystals. *Nature* **2014**, *506*, 208–211.
- (49) Archer, A. J.; Rucklidge, A. M.; Knobloch, E. Quasicrystalline Order and a Crystal-Liquid State in a Soft-Core Fluid. *Phys. Rev. Lett.* **2013**, *111*, 1–5.
- (50) Torquato, S. Inverse Optimization Techniques for Targeted Self-Assembly. *Soft Matter* **2009**, *5*, 1157.
- (51) O'Guz, E. C.; Mijailovi, A.; Schmiedeberg, M. Self-Assembly of Complex Structures in Colloid-Polymer Mixtures. **2017**, 1–13.
- (52) Gabriëse, A.; Löwen, H.; Smallenburg, F. Low-Temperature Crystal Structures of the Hard Core Square Shoulder Model. *Materials (Basel)*. **2017**, *10*.
- (53) Rey, M.; Law, A. D.; Buzza, D. M. A.; Vogel, N. Anisotropic Self-Assembly from Isotropic Colloidal Building Blocks. *J. Am. Chem. Soc.* **2017**, *139*, 17464–17473.
- (54) Louis, A. A.; Allahyarov, E.; Löwen, H.; Roth, R. Effective Forces in Colloidal Mixtures: From Depletion Attraction to Accumulation Repulsion. *Phys. Rev. E - Stat. Nonlinear, Soft Matter Phys.* **2002**, *65*, 1–11.
- (55) Rager, T.; Meyer, W. H.; Wegner, G.; Mathauer, K.; Machtle, W.; Schrof, W.; Urban, D. Block Copolymer Micelles as Seed in Emulsion Polymerization. *Macromol. Chem. Phys.* **1999**, *200*, 1681–1691.

- (56) Rey, M.; Fernández-Rodríguez, M. Á.; Steinacher, M.; Scheidegger, L.; Geisel, K.; Richtering, W.; Squires, T. M.; Isa, L. Isostructural Solid–solid Phase Transition in Monolayers of Soft Core–shell Particles at Fluid Interfaces: Structure and Mechanics. *Soft Matter* **2016**, *12*, 3545–3557.
- (57) Rey, M.; Hou, X.; Tang, J. S. J.; Vogel, N. Interfacial Arrangement and Phase Transitions of PNIPAm Microgels with Different Crosslinking Density. *Soft Matter* **2017**, *13*, 8717–8727.
- (58) Scheidegger, L.; Fernández-Rodríguez, M. Á.; Geisel, K.; Zanini, M.; Elnathan, R.; Richtering, W.; Isa, L. Compression and Deposition of Microgel Monolayers from Fluid Interfaces: Particle Size Effects on Interface Microstructure and Nanolithography. *Phys. Chem. Chem. Phys.* **2017**, *19*, 8671–8680.
- (59) Fulda, K. -U; Tieke, B. Langmuir Films of Monodisperse 0.5 Mm Spherical Polymer Particles with a Hydrophobic Core and a Hydrophilic Shell. *Adv. Mater.* **1994**, *6*, 288–290.
- (60) Fulda, K. U.; Tieke, B. Monolayers of Mono- and Bidisperse Spherical Polymer Particles at the Air/water Interface and Langmuir-Blodgett Layers on Solid Substrates. *Supramol. Sci.* **1997**, *4*, 265–273.
- (61) Vogel, N.; De Viguerie, L.; Jonas, U.; Weiss, C. K.; Landfester, K. Wafer-Scale Fabrication of Ordered Binary Colloidal Monolayers with Adjustable Stoichiometries. *Adv. Funct. Mater.* **2011**, *21*, 3064–3073.
- (62) Zell, Z. A.; Nowbahar, A.; Mansard, V.; Leal, L. G.; Deshmukh, S. S.; Mecca, J. M.; Tucker, C. J.; Squires, T. M. Surface Shear Inviscidty of Soluble Surfactants. *Proc. Natl. Acad. Sci.* **2014**, *111*, 3677–3682.

- (63) Fisher, S.; Kunin, R. Effect of Cross-Linking on the Properties of Carboxylic Polymers. I. Apparent Dissociation Constants of Acrylic and Methacrylic Acid Polymers. *J. Phys. Chem.* **1956**, *60*, 1030–1032.
- (64) Pepicelli, M.; Vervijlen, T.; Tervoort, T. A.; Vermant. Characterization and Modelling of Langmuir Interfaces with Finite Elasticity. *Soft Matter* **2017**, *13*, 5977–5990.
- (65) Sharma, V.; Jaishankar, A.; Wang, Y. C.; McKinley, G. H. Rheology of Globular Proteins: Apparent Yield Stress, High Shear Rate Viscosity and Interfacial Viscoelasticity of Bovine Serum Albumin Solutions. *Soft Matter* **2011**, *7*, 5150–5160.
- (66) Graham, D. E.; Phillips, M. C. Proteins at Liquid Interfaces II. Adsorption Isotherms. *J. Colloid Interface Sci.* **1979**, *70*, 415–426.
- (67) Svitova, T. F.; Wetherbee, M. J.; Radke, C. J. Dynamics of Surfactant Sorption at the Air/water Interface: Continuous-Flow Tensiometry. *J. Colloid Interface Sci.* **2003**, *261*, 170–179.
- (68) Rauh, A.; Rey, M.; Barbera, L.; Zanini, M.; Karg, M.; Isa, L. Compression of Hard Core-Soft Shell Nanoparticles at Liquid-Liquid Interfaces: Influence of the Shell Thickness. *Soft Matter* **2016**, *13*, 158–169.
- (69) Vogel, N.; Fernández-López, C.; Pérez-Juste, J.; Liz-Marzán, L. M.; Landfester, K.; Weiss, C. K. Ordered Arrays of Gold Nanostructures from Interfacially Assembled Au@ PNIPAM Hybrid Nanoparticles. *Langmuir* **2012**, *28*, 8985–8993.

TOC

